

the electron is *on the average* at rest, that is the rest frame of \bar{p} ; we regard a monochromatic beam as the limit of a wave train of finite duration, and use the laboratory frame in which the electron is at rest before the arrival of the beam, that is the rest frame of p . The wavelength shift arises, in fact, from the Lorentz

transformation from the rest frame of \bar{p} to the laboratory frame. It is therefore of crucial importance to distinguish clearly between these frames.

We wish to thank Dr. P. Auvil for helpful discussions of the material in this Appendix.

High-Magnetic-Field Specific Heat of a Low-Dislocation-Density Alloy Superconductor*

R. R. HAKE

Atomics International Division of North American Aviation, Inc., Canoga Park, California

AND

W. G. BRAMMER

North American Aviation Science Center, Canoga Park, California

(Received 5 August 1963; revised manuscript received 21 October 1963)

The specific heat C of a *well-annealed* alloy V-5 at.% Ta, measured at $1.4 \leq T \leq 5^\circ\text{K}$ in steady magnetic fields, displays sharp, bulk, superconducting transitions at upper critical fields H_{c2} a factor ≈ 10 larger than the calorimetrically derived thermodynamic critical fields H_c . The transitions are similar to those observed earlier by Morin *et al.*¹ in V_3Ga , but in the present case it is unlikely that the bulk nature of the high-field transitions can be attributed to a nearly complete occupation of the specimen volume by dislocation-centered high-field superconducting filaments of diameter comparable to the penetration depth, since electron transmission microscopy studies on an identically prepared specimen indicate that in at least 95% of the specimen volume the mean separation between dislocations is greater than 1.4×10^{-4} cm. However, the present data are explicable on the basis of the Ginzburg-Landau-Abrikosov-Gor'kov theory with a parameter $\kappa \approx H_{c2}/\sqrt{2}H_c \approx 7$. The transition specific heat jumps $\Delta C(T_s)/\gamma T_s = 1.44, 1.15, 1.10, 0.94$ occur at $T_s = 4.30, 4.09, 3.85, 3.37^\circ\text{K}$ in fields $H = 0, 1, 2, 4$ kG, respectively, where $\gamma =$ normal state electronic specific heat coefficient $= 9.20$ mJ/mole $(\text{K}^\circ)^2$. The $\Delta C(T_s)$ values are in fair agreement with those calculated via Ehrenfest's equation for second-order phase transitions using Abrikosov's theoretical value of $(\partial I/\partial H)_T$ at T_s for $\kappa = 7$, where $I =$ magnetization. For $(T_s/T) \geq 1.8$, $C_{es}/\gamma T_s = a \exp(-bT_s/T)$ with $a = 8.95, 6.24, 5.01, 4.7$; $b = 1.48, 1.28, 1.17, 1.1$; for $H = 0, 1, 2, 4$ kG, respectively, where C_{es} is the electronic contribution to the specific heat. The exponential temperature dependence of C_{es} down to 1.4°K suggests an essentially everywhere finite, field-dependent, high-field energy gap in accord with Abrikosov's vortex model.

RECENT calorimetric measurements of Morin *et al.*¹ revealed bulk, reversible, second-order superconducting transitions in V_3Ga at magnetic fields much larger than the thermodynamic critical fields. The surprising bulk nature of the high-field transitions was attributed^{1,2} to a nearly complete occupation of the specimen volume by dislocation-centered high-field superconducting *filaments* of diameter comparable to a penetration depth $\lambda \approx 5 \times 10^{-6}$ cm,³ requiring a high dislocation density $\approx 4 \times 10^{10}$ cm⁻².² On the other hand, it was suggested^{4,5} that the transitions in V_3Ga might be the

thermodynamic manifestation of a "second kind" of *superconductivity* explicable on the basis of the spatially uniform negative-surface-energy theories of Ginzburg, Landau, Abrikosov, and Gor'kov (GLAG)⁶⁻¹⁰ or of Goodman.^{11,12} The present measurements offer strong support for the negative-surface-energy interpretation since high-field bulk-superconducting calorimetric transitions are observed for a solid-solution bcc superconducting alloy, V-5 at.% Ta, which, after arc melting, was annealed for 2 h at 1600°C (0.85 of the melting

* This research was supported in part by the U. S. Atomic Energy Commission.

¹ F. J. Morin, J. P. Maita, H. J. Williams, R. C. Sherwood, J. H. Wernick, and J. E. Kunzler, *Phys. Rev. Letters* **8**, 275 (1962).

² J. J. Hauser and E. Helfand, *Phys. Rev.* **127**, 386 (1962).

³ For a discussion of the thermodynamic arguments for high critical fields in specimens of dimension $\approx \lambda$ see, for example, D. Shoenberg, *Superconductivity* (Cambridge University Press, Cambridge, England, 1952), p. 171.

⁴ B. B. Goodman, *Phys. Letters* **1**, 215 (1962).

⁵ T. G. Berlincourt and R. R. Hake, *Phys. Rev. Letters* **9**, 293 (1962).

⁶ V. L. Ginzburg and L. D. Landau, *Zh. Eksperim. i Teor. Fiz.* **20**, 1064 (1950); *V. L. Ginzburg, Nuovo Cimento* **2**, 1234 (1955).

⁷ A. A. Abrikosov, *Zh. Eksperim. i Teor. Fiz.* **32**, 1442 (1957) [translation: *Soviet Phys.—JETP* **5**, 1174 (1957)].

⁸ L. P. Gor'kov, *Zh. Eksperim. i Teor. Fiz.* **37**, 1407 (1959) [translation: *Soviet Phys.—JETP* **10**, 998 (1960)].

⁹ L. P. Gor'kov, *Zh. Eksperim. i Teor. Fiz.* **37**, 835 (1950) [translation: *Soviet Phys.—JETP* **10**, 593 (1960)].

¹⁰ For a recent discussion of experimental evidence bearing on the GLAG theory see T. G. Berlincourt and R. R. Hake, *Phys. Rev.* **131**, 140 (1963).

¹¹ B. B. Goodman, *Phys. Rev. Letters* **6**, 597 (1961).

¹² B. B. Goodman, *IBM J. Res. Develop.* **6**, 63 (1962).

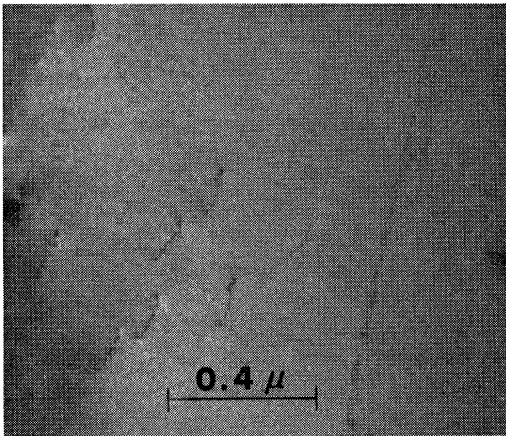


FIG. 1. Transmission electron micrograph of $\approx 1000\text{-\AA}$ -thick foil of V-5 at.% Ta prepared from a specimen arc melted and annealed in a manner identical to that employed for the calorimetric specimen. Several dislocations (average density $\approx 10^9\text{ cm}^{-2}$) and a portion of a small-angle subgrain boundary can be seen in this micrograph which typifies those few isolated regions outside grain and subgrain boundaries which were found to contain dislocations. Such atypical dislocation-rich regions are estimated to comprise less than 5% of the total specimen volume; the remaining 95% of the typical subgrain area over which no dislocations whatsoever could be detected by the electron transmission microscope is estimated to contain a dislocation density of less than $5 \times 10^7\text{ cm}^{-2}$.

point) and then slowly cooled so as to produce large grains of 1 mm^2 average cross section, which, over at least 95% of their area, contain an average dislocation density of less than $5 \times 10^7\text{ cm}^{-2}$ as estimated from electron transmission microscopy studies.

Figure 1 is a transmission electron micrograph of the well-annealed V-5 at.% Ta showing the typical appearance of those few atypical regions outside grain or subgrain boundaries which were found to contain resolvable dislocations. Thin foils for the dislocation studies were prepared by electrochemical and chemical thinning of strips cut (and then polished from 0.035 to 0.005 in.) from a V-5 at.% Ta specimen, arc melted and annealed in a manner identical to that employed for the calorimetric specimen. Individual grains were observed to contain subgrains of $\approx 200\ \mu$ average diameter. Cuts through the subgrain boundaries usually revealed regular and nearly parallel arrays of dislocations of average density $\approx 10^{11}\text{ cm}^{-2}$, but subgrain boundaries are narrow ($\approx 0.1\ \mu$) and hence constitute only $\approx 0.15\%$ of the total specimen volume. Aside from the subgrain boundaries, the isolated, atypical, dislocation-rich regions typified by Fig. 1 were found to contain dislocation densities of $1-3 \times 10^9\text{ cm}^{-2}$ as estimated using the random line intersection method¹³ on 10 micrographs of such areas taken at $50\ 000\times$. It is possible that these dislocations were introduced during preparation of the thin foil specimens. Foils were tilted during the electron transmission examinations to provide various contrast conditions and thus ensure that essentially all of the

dislocations were observed. Over at least 95% of the typical subgrain area, exclusive of boundaries, no dislocations whatsoever could be observed. An estimation of the extent that dislocations might remain undetected leads to an upper limit of $5 \times 10^7\text{ cm}^{-2}$ in these apparently dislocation-free areas. Hence the mean separation between dislocations in at least 95% of the specimen volume is estimated to be greater than $1.4 \times 10^{-4}\text{ cm}$, much larger than the usual penetration depths.

Figure 2 shows the specific heat C of the well-annealed V-5 at.% Ta specimen, measured at $1.4 \leq T \leq 5^\circ\text{K}$ in fields $H=0, 0.5, 1, 2, 3, 4\text{ kG}$, and plotted in the usual (C/T) versus T^2 form. The apparatus, technique, and data reduction are essentially the same as previously described.¹⁴ Magnetic fields were generated by a 3-in.-i.d. Nb-Zr wire superconducting Helmholtz-pair solenoid with a field homogeneity $\approx 0.2\%$ over the specimen volume. The close agreement at equal (H, T) of points with different (H, T) history (see figure caption) is in contrast to expectations based on a high-field-filamentary-mesh model.^{15,16} However, some residual flux trapping probably occurred in the $8.5 < T^2 < 18$ ($^\circ\text{K}$)² region after application of a 4 kG field at lower temperature, as indicated by the $\approx 1\%$ mismatch of points with and without ticks for $H=0$ in that temperature range.

The midpoints of the negative slope intervals $\Delta T \approx 0.08\text{ K}^\circ$ define superconducting transition temperatures $T_s(H)$. As for V_3Ga ,¹ a large specific-heat jump $\Delta C(T_s)$ persists for this relatively low dislocation-density specimen in magnetic fields large in comparison with the calorimetrically derived thermodynamic critical fields [$H_c(T=0) \equiv H_0 = 1.11\text{ kG}$]. Table I summarizes the superconducting transition characteristics. The $\Delta C(H=0)$ value is in good agreement with the $1.43\gamma T_s$ predicted by the BCS theory.¹⁷

In the normal state above $T_s(H)$ all the (C/T) versus T^2 curves of Fig. 2 superimpose on a straight line, indicating that the usual normal state relationship $C_n = \gamma T + \beta T^3$ is obeyed independent of H . Here $\gamma \equiv$ electronic specific heat coefficient $= 9.20 \pm 0.02\text{ mJ/mole}(\text{K}^\circ)^2$ and $\beta^{-1/3} \propto \theta_D \equiv$ Debye temperature $= 357 \pm 2.5^\circ\text{K}$, where the probable errors as given by the least squares analysis are indicated.

Below $T_s(H)$ all the C/T versus T^2 curves of Fig. 2 drop rapidly with decrease of T , suggesting pure superconducting-state energy-gap behavior even in high

¹⁴ R. R. Hake, Phys. Rev. **123**, 1986 (1961).

¹⁵ K. Mendelssohn, Proc. Roy. Soc. (London) **A152**, 34 (1935). The nearly complete suppression of superconductivity observed calorimetrically by Mendelssohn and Moore in Sn-4% Bi after "switching on and off a high-field at the lowest temperature" probably indicates specimen inhomogeneity sufficient to create a true flux-trapping high-field-filamentary-mesh in an otherwise low upper critical field material.

¹⁶ C. P. Bean, Phys. Rev. Letters **8**, 250 (1962).

¹⁷ J. Bardeen, L. N. Cooper, and J. R. Schrieffer, Phys. Rev. **108**, 1175 (1957); J. Bardeen and J. R. Schrieffer in *Progress in Low Temperature Physics*, edited by C. J. Gorter (Interscience Publishers, Inc., New York, 1961), Vol. III, p. 170.

¹³ R. K. Ham, Phil. Mag. **6**, 1183 (1961).

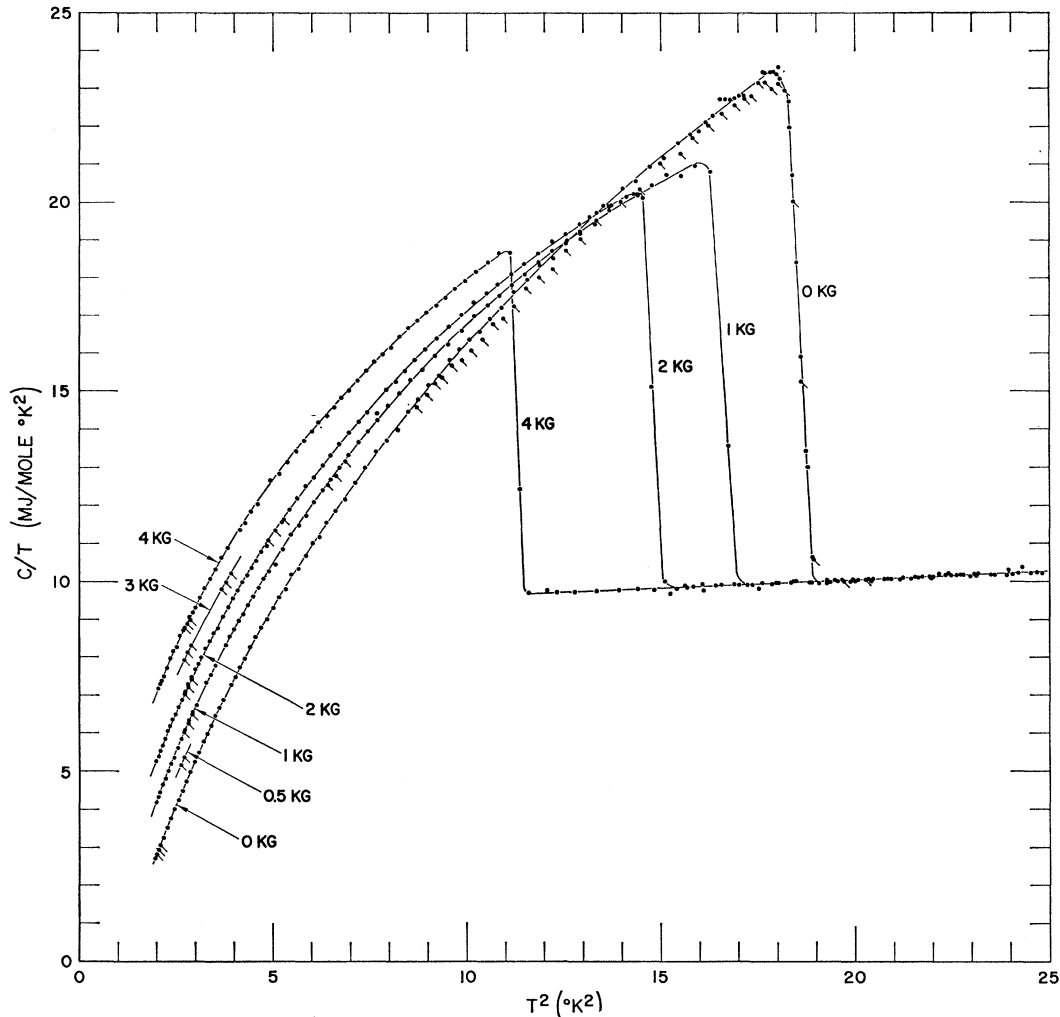


Fig. 2. Specific heat C of well-annealed V-5 at. % Ta plotted as (C/T) versus T^2 . All points were taken at constant H with increasing T . Solid circles for $H=0$ represent measurements on the virgin sample prior to magnetic field application. Solid circles for $H=1, 2, 4$, kG were taken after applying H in the normal state at about 5.5°K and then cooling via a mechanical heat switch to 1.4°K in the presence of the field. Solid circles with ticks for various H were all taken in succession after cooling from about 5.5 to 1.4°K in zero field.

magnetic fields. Figure 3 shows $\log_{10}(C_{es}/\gamma T_s)$ versus (T_s/T) , where C_{es} is the electronic contribution to the specific heat for $T < T_s(H)$. For $(T_s/T) \gtrsim 1.8$ the linearity of the curves of Fig. 2 indicates the validity of a superconducting-state energy-gap expression

$$C_{es}(H, T)/\gamma T_s(H) = a(H) \exp[-b(H)T_s(H)/T], \quad (1)$$

with $a=8.95, 6.24, 5.01, 4.7$ and $b=1.48, 1.28, 1.17, 1.1$ for $H=0, 1, 2, 4$ kG. For $H=0$ the (a, b) values are close to those observed for other transition metal alloys in the same region of reduced temperature,^{14,18} and in fair agreement with the $(a=8.5, b=1.44)$ of BCS.¹⁷

The calorimetric data allow an estimate of the entropy

change at $T_s(H)$. For the normal state

$$S_n(T) = \int_0^T (C_n/T) dT = \gamma T + \beta T^3/3. \quad (2)$$

For the "superconducting state" at $T \lesssim T_s(H)$ and at constant H

$$S_s(T) = \int_0^{T=1.4} \{ [C_{es}(H, T) + \beta T^3]/T \} dT + \int_{T=1.4}^T [C_s(H, T)/T] dT, \quad (3)$$

where $C_{es}(H, T \leq 1.4^\circ\text{K})$ is approximated by Eq. (1) with (a, b) values as derived from data at $T > 1.4^\circ\text{K}$, and the second integral is obtained by numerical integra-

¹⁸ C. H. Cheng, K. P. Gupta, E. C. van Reuth, and P. A. Beck, Phys. Rev. **126**, 2030 (1962).

TABLE I. Superconducting transition characteristics of V-5 at.% Ta.

Applied H (or H_{c2}^a at $T=T_s^b$) (kG)	T_s^b (°K)	ΔC^c (mj/mole K°)	$\Delta C^c/(\gamma T_s)^d$	H_{c2}^e (kG)	$H_{c2}/\sqrt{2}H_e$ $\approx \kappa^f$	ΔC^g (GLAG) (mj/mole K°)
0	4.30	57	1.44	0	...	58
1	4.09	43	1.15	0.101	7.0	50
2	3.85	39	1.10	0.205	6.9	42
4	3.37	29	0.94	0.400	7.0	28

^a Measured upper critical field.

^b Measured superconducting transition temperature.

^c Measured specific heat jump.

^d (γT_s) is the normal state electronic specific heat at T_s .

^e Thermodynamic critical field derived from calorimetric data.

^f GLAG parameter.

^g Specific-heat jump calculated by means of the GLAG theory and Ehrenfest's equations.

tion. Eqs. (2) and (3) yield $[S_n(T_s) - S_s(T_s)]/S_n(T_s) = 0.001, 0.02, 0.04, 0.08$ for $H=0, 1, 2, 4$ kG. Judging from the small $\Delta S(T_s, H=1$ kG), it seems likely that the actual entropy change at T_s in high fields is zero (second-order transition) or very small, as for $V_3\text{Ga}$.¹ The divergence of $\Delta S(T_s)/S_n(T_s)$ from zero as H increases probably indicates that $C_{es}(T < 1.4^\circ\text{K}, H \geq 1$ kG) is greater than the exponential extrapolation [Eq. (1)] used in Eq. (3). Equations (2) and (3) and standard thermodynamic relationships¹⁹ also yield the *thermodynamic* critical field $H_c(T) \approx H_0[1 - (T/T_c)^2]$ with $H_0 = 1.11$ kG and $T_c = 4.30^\circ\text{K}$. The deviation¹⁹ $D(T) = \{H_c(T) - H_0[1 - (T/T_c)^2]\}/H_0$ has a maximum negative value -0.03 , close to the BCS prediction. The $H_c(T_s)$ values are listed in Table I.

The present calorimetric data are in fair accord with several predictions of the GLAG theory:

(1) *Magnitude of the specific-heat jump.* According to GLAG the high-field superconducting state persists up to the critical values (T_s, H_{c2}) where flux penetration is complete and a second-order transition to the normal state occurs. Assuming that the transition at $T_s(H)$ is indeed second order, Ehrenfest's equations can be applied⁴:

$$\Delta C(T_s) = VT_s(\partial I/\partial H)_{T_s}(dH_{c2}/dT)^2_{T_s}, \quad (4)$$

where ΔC is the molar specific heat jump, $V \equiv$ atomic volume ≈ 8.44 cm³/mole, and I is the high-field superconducting state magnetization. For $(\partial I/\partial H)_{T_s}$ we take Abrikosov's⁷ theoretical value $[1.18(2\kappa^2 - 1)(4\pi)]^{-1} = 6.9 \times 10^{-4}$ [for $\kappa = 7$ as derived from Eq. (5) below]. We obtain $(dH_{c2}/dT)_{T_s}$ by differentiating the expression $H_{c2} = 10.4$ kG $[1 - (T/4.30^\circ\text{K})^2]$ which fits the four (H_{c2}, T) points of Table I to within 1.5%. The $\Delta C(T_s)$ values thus calculated from Eq. (4) are listed in Table I and are in fair accord with the measured values.

(2). *Magnitude of the upper critical field H_{c2} .* According to GLAG, near T_c

$$H_{c2} = \sqrt{2}\kappa H_e. \quad (5)$$

Over the present temperature range of H_{c2} determinations Eq. (5) should hold to within 10% regardless of the present theoretical uncertainty in $H_{c2}(T)$. The parameter κ is given by the Gor'kov-Goodman formula^{8,12,20}

$$\kappa = \kappa_0 + 7.5 \times 10^3 \rho_n \gamma^{1/2}, \quad (6)$$

where for the present alloy $\kappa_0 = 0.31(S/S_f)^{-2}$, $\rho_n \equiv$ normal

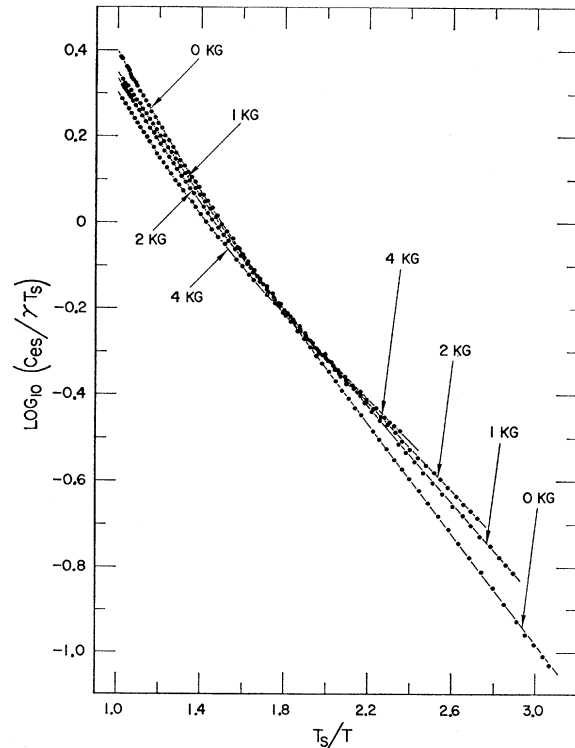


Fig. 3. The reduced electronic specific heat $C_{es}/\gamma T_s$ versus (T_s/T) for well-annealed V-5 at.% Ta in various applied fields H at temperatures below the superconducting transitions $T_s(H)$. The linearity of the curves for $(T_s/T) \gtrsim 1.8$ implies the validity of an energy gap expression [Eq. (1)].

¹⁹ See, for example, D. E. Mapother, IBM J. Res. Develop. 6, 77 (1962); Phys. Rev. 126, 2021 (1962).

²⁰ L. P. Gor'kov, Zh. Eksperim. i Teor. Fiz. 36, 1918 (1959) [translation: Soviet Phys.—JETP 9, 1364 (1959)].

state resistivity $= 5.7 \times 10^{-6} \Omega\text{cm}$, $\gamma = 1.1 \times 10^4$ ergs/cm³ (K^o)², and (S/S_f) is the ratio of the free Fermi surface area to that of a corresponding free electron gas. Making the usual^{10,11} rather uncertain assumption $(S/S_f) \approx 0.6$ for transition metals, Eq. (6) yields $\kappa \approx 0.86 + 4.49 = 5.35$ in fair agreement with the κ values based on Eq. (5) and listed in Table I.

(3). *High-field energy gap.* According to Abrikosov⁷ the high-field superconducting state consists of a regular lattice of quantized supercurrent vortices over which the field-dependent Ginzburg-Landau order parameter [hence BCS energy gap $\epsilon(H)$ ^{8,20}] varies, becoming zero only along (zero-volume) lines at the center of each vortex where H is a maximum. The high-field superconducting-state electronic specific heat $C_{es}(T, H)$ might then be expected to reflect a spatially averaged gap $\bar{\epsilon}(H)$ which diminishes with increasing H , as is indeed implied by the observed $C_{es}(T, H)$ of Eq. (1) since $\bar{\epsilon}(H) \approx 2b(H)kT_s(H)$,²¹ where k is the Boltzmann constant. In analogy with the case of pure element gap anisotropy in momentum space,^{22,23} one might expect the smaller

gap regions in real space (assuming Abrikosov's model⁷) to dominate $C_{es}(T, H \gg 0)$ at very low reduced temperature, producing considerable upward curvature in the plots of Fig. 3 at higher (T_s/T) , as is also suggested by the entropy considerations above, and which might account for the failure of the V₃Ga¹ high-field (C/T) versus T^2 curves to extrapolate to 0 at $T^2 = 0$.

Note added in proof. For a derivation of entropy, Gibbs free energy, and magnetization from the present specific-heat data see R. R. Hake, Rev. Mod. Phys. **36**, 124 (1964). The magnetization and its relationship to the effective field-dependent energy gap (as inferred from the exponential temperature dependence of the high-field superconducting-state electronic specific heat) appear to be in reasonable accord with the GLAG theory.

ACKNOWLEDGMENTS

We wish to thank D. M. Sellman and H. Nadler for specimen preparation, C. G. Rhodes for micrographic examinations, and K. Medeiros for computer programming. Valuable discussions with T. G. Berlincourt, D. Kramer, H. B. Levine, and H. W. Wiedersich are gratefully acknowledged.

²¹ See, for example, E. A. Lynton, *Superconductivity* (Methuen and Company, Ltd., London, 1962), p. 84.

²² L. N. Cooper, Phys. Rev. Letters **3**, 17 (1959).

²³ P. W. Anderson, J. Phys. Chem. Solids **11**, 26 (1959).

Faraday Rotation of Rare-Earth (III) Phosphate Glasses

S. B. BERGER,† C. B. RUBINSTEIN, C. R. KURKJIAN, AND A. W. TREPTOW
Bell Telephone Laboratories, Murray Hill, New Jersey

(Received 25 April 1963; revised manuscript received 17 September 1963)

The optical Faraday rotation of trivalent rare-earth phosphate glasses has been investigated at room temperature. The rotation is ascribed primarily to strong electric dipole transitions involving the rare-earth 4f electrons and is described as a function of the incident light wavelength by a simplified equation involving an effective transition wavelength. The linear dependence of the rotation on the concentration is experimentally demonstrated. The relative magnitudes of the magnetic rotation of the rare-earth ions are compared to the quantity p^2/g , where p is the effective magneton number and g is the spectroscopic splitting factor. This comparison demonstrates the importance of the other parameters, especially the transition wavelengths and electric dipole matrix elements. It also indicates that a prediction of relative rotations of ions, molecules, etc., on the basis of relative magnitudes of magnetic susceptibility and concentration alone is not meaningful.

INTRODUCTION

FARADAY rotation of some rare-earth ions has been extensively studied at Leiden University, especially by J. Becquerel, in the first half of this century.¹ The object of that effort was to understand the phenomena of Faraday rotation with particular respect to its wavelength dependence, temperature dependence, and relation to the magnetic susceptibility.

The object of this paper is to present the room-temperature optical Faraday rotation of all the trivalent rare-earth ions (except Pm³⁺) in the isotropic phosphate glass matrix as a function of wavelength and concentration in order to furnish a basis for numerical comparison of the magnetic rotatabilities of the trivalent rare-earth ions. The results indicate that the relative magnitudes of the observed rotations bear no simple relation to any one parameter. For example, the magnetic susceptibility is shown not to be a suitable basis for the prediction of the relative rotations. However, the experimental evidence is that the wavelength

† Present address: RCA Laboratories, Princeton, New Jersey.

¹ Communications Kamerlingh Onnes Laboratory, Leiden University, especially during the period 1925-1936.

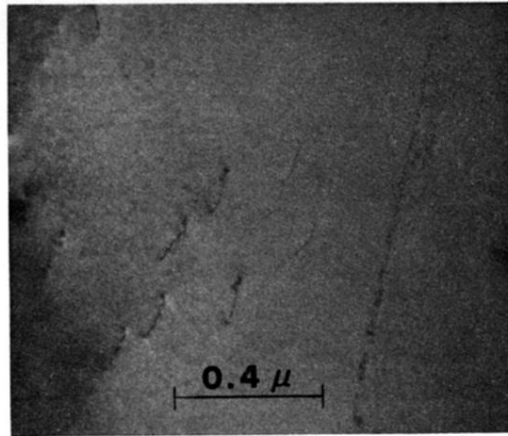


FIG. 1. Transmission electron micrograph of $\approx 1000\text{-\AA}$ -thick foil of V-5 at.% Ta prepared from a specimen arc melted and annealed in a manner identical to that employed for the calorimetric specimen. Several dislocations (average density $\approx 10^9\text{ cm}^{-2}$) and a portion of a small-angle subgrain boundary can be seen in this micrograph which typifies those few isolated regions outside grain and subgrain boundaries which were found to contain dislocations. Such atypical dislocation-rich regions are estimated to comprise less than 5% of the total specimen volume; the remaining 95% of the typical subgrain area over which no dislocations whatsoever could be detected by the electron transmission microscope is estimated to contain a dislocation density of less than $5 \times 10^7\text{ cm}^{-2}$.